

AD-A224 325

DTIC FILE COPY

OFFICE OF NAVAL RESEARCH

Contract No.: N00014-90-J-1119

R&T Code: 413f008

TECHNICAL REPORT NO. 4

Microscopic Aspects of the Initial Stages of Epitaxial Growth.
A Scanning Tunneling Microscopy Study
of Si on Si(001)

by

M. G. Lagally, Y.-W. Mo, R. Kariotis, B. S. Swartzentruber,
and M. B. Webb
Department of Materials Science and Engineering
University of Wisconsin-Madison
Madison, WI 53706

April 1, 1990

DTIC
ELECTE
JUL 02 1990
S B D

Kinetics of Ordering and Growth at Surfaces,
ed. M. G. Lagally, Plenum, 1990 (in press)

Reproduction in whole or in part is permitted
for any purpose of the United States Government

DISTRIBUTION OF THIS DOCUMENT IS UNLIMITED

41 28 29 018

SECURITY CLASSIFICATION OF THIS PAGE

REPORT DOCUMENTATION PAGE

1a. REPORT SECURITY CLASSIFICATION Unclassified			1b. RESTRICTIVE MARKINGS N/A		
2a. SECURITY CLASSIFICATION AUTHORITY N/A			3. DISTRIBUTION/AVAILABILITY OF REPORT		
2b. DECLASSIFICATION/DOWNGRADING SCHEDULE N/A			Approved for public release; distribution unlimited.		
4. PERFORMING ORGANIZATION REPORT NUMBER(S) N00014-90-J-1119-04			5. MONITORING ORGANIZATION REPORT NUMBER(S)		
6a. NAME OF PERFORMING ORGANIZATION Board of Regents of the University of Wisconsin-Madison		6b. OFFICE SYMBOL (If applicable)	7a. NAME OF MONITORING ORGANIZATION Office of Naval Research Branch Office Chicago		
6c. ADDRESS (City, State, and ZIP Code) 750 University Avenue Madison, WI 53706			7b. ADDRESS (City, State, and ZIP Code) 536 S. Clark Street Chicago, IL 60605		
8a. NAME OF FUNDING/SPONSORING ORGANIZATION Office of Naval Research--Chemistry Program		8b. OFFICE SYMBOL (If applicable)	9. PROCUREMENT INSTRUMENT IDENTIFICATION NUMBER N00014-90-J-1119-04		
8c. ADDRESS (City, State, and ZIP Code) 800 N. Quincy Street Arlington, VA 22217			10. SOURCE OF FUNDING NUMBERS		
			PROGRAM ELEMENT NO.	PROJECT NO.	TASK NO.
			WORK UNIT ACCESSION NO.		
11. TITLE (Include Security Classification) Microscopic Aspects of the Initial Stages of Epitaxial Growth. A Scanning Tunneling Microscopy Study of Si on Si(001)					
12. PERSONAL AUTHOR(S) M. G. Lagally, Y.-W. Mo, R. Kariotis, B. S. Swartzentruber, and M. B. Webb					
13a. TYPE OF REPORT		13b. TIME COVERED FROM _____ TO _____		14. DATE OF REPORT (Year, Month, Day) April 1, 1990	
				15. PAGE COUNT 24	
16. SUPPLEMENTARY NOTATION Kinetics of Ordering and Growth at Surface, ed. M. G. Lagally, Plenum 1990 (in press)					
COSATI CODES			18. SUBJECT TERMS (Continue on reverse if necessary and identify by block number)		
FIELD	GROUP	SUB-GROUP	Surfaces, kinetics, ordering, growth, STM, diffusion, Si, Ge		
19. ABSTRACT (Continue on reverse if necessary and identify by block number)					

Scanning tunneling microscopy offers the opportunity to investigate growth and ordering processes at the atomic level and hence to identify and distinguish different kinetic and energetic mechanisms that may be operative. A review of the fundamental mechanisms of growth is given. Scanning tunneling microscopy measurements of the ordering and growth of Si on Si(001) are used to illustrate these mechanisms. Diffusion coefficients, growth anisotropy and lateral accommodation coefficients, equilibrium island shapes and free energies, edge desorption energies, and diffusional anisotropy are discussed.

20. DISTRIBUTION/AVAILABILITY OF ABSTRACT <input type="checkbox"/> UNCLASSIFIED/UNLIMITED <input checked="" type="checkbox"/> SAME AS RPT. <input type="checkbox"/> DTIC USERS			21. ABSTRACT SECURITY CLASSIFICATION Unclassified		
22a. NAME OF RESPONSIBLE INDIVIDUAL Max G. Lagally			22b. TELEPHONE (Include Area Code) 608-263-2078		22c. OFFICE SYMBOL

MICROSCOPIC ASPECTS OF THE INITIAL STAGES OF EPITAXIAL GROWTH:

A SCANNING TUNNELING MICROSCOPY STUDY OF Si ON Si(001)

M. G. Lagally, Y.-W. Mo, R. Kariotis,
B. S. Swartzentruber, and M. B. Webb

University of Wisconsin-Madison
Madison, WI 53706 USA

ABSTRACT

Scanning tunneling microscopy offers the opportunity to investigate growth and ordering processes at the atomic level and hence to identify and distinguish different kinetic and energetic mechanisms that may be operative. A review of the fundamental mechanisms of growth is given. Scanning tunneling microscopy measurements of the ordering and growth of Si on Si(001) are used to illustrate these mechanisms. Diffusion coefficients, growth anisotropy and lateral accommodation coefficients, equilibrium island shapes and free energies, edge desorption energies, and diffusional anisotropy are discussed.

INTRODUCTION

Carefully engineered growth of crystals through atomistic processes like molecular beam epitaxy (MBE), chemical vapor deposition (CVD), or variants on these has formed the basis of a large and still expanding technology. Although many exotic devices have been developed, frequently by empiricism, much is still not understood, in particular about the kinetics of growth and about the interactions between atoms that control the kinetics and thermodynamics of growth. The lack of such understanding is becoming more evident with the attempts to develop atomistic-scale structures, such as ones based on vicinal substrates or on a particular distribution of defects in surfaces. Because of the microscopic view that it affords, scanning tunneling microscopy provides an excellent opportunity to investigate in a quantitative manner atomistic processes during growth. In this article, we briefly review basic aspects of the kinetics of growth at the atomic level and illustrate these with examples taken from STM measurements of Si on Si(001).

The theoretical framework for investigating crystal growth has been in hand for a long time, and has, in some cases, been developed to a considerable degree.¹⁻⁵ Consider the simplest case: the homoepitaxial growth of material on itself (A-on-A). Atoms arrive from the vapor phase at a surface. To remain on the surface ("accommodate") they must give up their heat of condensation through one or a series of inelastic collisions. Once bound in the holding potential of the surface, an atom

will diffuse until it finds another of its kind, either at the edge of a terrace or another freely diffusing atom. In the latter case, a critical nucleus may form, which will grow with the addition of a third atom. On a surface of a material with strong bonding, two atoms may actually form already a stable nucleus. Nucleation is thus the first stage, followed subsequently by growth, and eventually by "coarsening" (or "ripening"). The growth and coarsening processes, and the influence of kinetic and thermodynamic factors on them, are now discussed in greater detail.

In any growth process, arriving atoms "like each other", i.e., they desire thermodynamically to form densely packed islands. Depending on the relative interfacial free energies⁴ of the adsorbate atoms and substrate, these islands may be three-dimensional (3D) clusters (Volmer-Weber growth), two-dimensional (2D) islands (Frank-van-der Merwe growth), or an intermediate situation (Stranski-Krastanov growth) in which an initial 2D layer is followed by 3D clusters. Clearly a homoepitaxial system desires to form 2D islands. The thermodynamics of all three cases can be described by a simple phase diagram illustrating phase coexistence (i.e., first-order phase transformations). The two phases are the islands and the "2-D vapor", which consists of those atoms (monomers) that are trapped in the holding potential of the surface but are not attached to islands. They represent the lateral vapor pressure of the islands at the temperature of the system. This vapor pressure is determined, as usual, through a Clausius-Clapeyron relation with the barrier being the effective lateral desorption energy of an atom from an island. (No equilibrium with the 3D vapor is assumed to exist). Figure 1 shows the relevant phase diagram. Below some transition temperature related to the cohesive energy of the island structure, 2D "solid" and 2D "vapor" coexist. The equilibrium concentration of each at a particular surface coverage and temperature is given by the phase boundaries at that temperature. Consider now a growth process. If the shutter from a deposition source is opened (and subsequently closed again) at sufficiently low temperature (below T_c), the coverage rapidly changes to some value inside the two-phase coexistence region through an increase in monomers, producing the equivalent of a random disordered phase quenched to a thermodynamic condition at which it is unstable ("chemical-potential" quench). The quench is shown by the horizontal arrow in Fig. 1. The disordered phase represents a condition of supersaturation of monomers, which then desire to attach themselves to existing islands or form new ones by nucleation. The process of island growth continues until the supersaturation is eliminated and islands are again in local 2D equilibrium with their vapor. As long as the supersaturation is maintained, all islands grow in an attempt to reduce the supersaturation (LeChatelier's Principle). MBE, or any other growth process, is simply a continuing series of chemical-potential quenches to maintain the supersaturation.

The most important microscopic quantity involved in the formation of stable nuclei and their growth is the diffusion coefficient for monomers on the surface at the surface temperature, consisting of an activation energy, E_{migr} , and a preexponential factor, D_0 , that involves the usual quantities of attempt frequency, geometric factors, and an entropy term. The transfer of the heat of condensation of the arriving atom to the lattice may influence the measurement of E_{migr} over a particular (low) temperature range (see below). Nucleation and growth are assumed to be unactivated. The growth rate of an island can then be simply written in terms of a flux to the island and a flux from the island:

$$r(T) \propto \nu_0 e^{-E_{migr}/kT} \left[1 - A e^{-E_{form}/kT} \right] \quad (1)$$

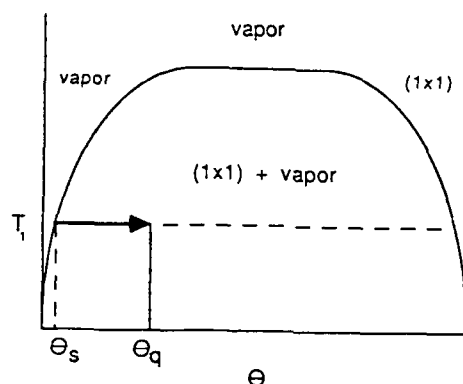


Fig. 1. Phase diagram of a lattice gas system in which two phases may coexist. At any temperature T_1 and coverages within the boundaries of the coexistence region, a solid phase (2D islands, here labeled (1x1)) coexists with a vapor at the appropriate concentration (the lateral vapor pressure), $\theta_s(T_1)$. The horizontal arrow indicates a chemical potential quench to a supersaturated state θ_q that will then decay by diffusion and island growth to the equilibrium state.

The flux from the island involves the creation of a diffusable species, with an activation energy, E_{form} , which represents the effective lateral desorption ("evaporation") energy of an atom from the island. The constant A is the preexponential factor for desorption (or more generally the ratio of desorption prefactor to accommodation coefficient). The attempt frequency, ν_0 , is explicitly shown. In a simple bond-breaking model (applicable reasonably well to metals), one expects the activation energy for self-diffusion, E_{migr} , to be of the order of 10% of the cohesive energy of the solid, and $E_{\text{form}} > E_{\text{migr}}$, because more bonds need to be broken to create a diffusable species. It is not certain how these numbers might differ for semiconductors, but it is possible that E_{migr} may actually be quite low.⁶ This conclusion arises from the concept that the minimum-energy path for the motion of a diffusing species does not involve the breaking and subsequent reforming of bonds, but rather involves some form of continuous charge transfer in going from the initial to the final site. In Volmer-Weber (i.e., B-on-A) growth, E_{form} may be less than E_{migr} .⁷ In the homoepitaxial system considered here, we expect, for any reasonable degree of supersaturation (in MBE, supersaturations are typically very large) that the flux away from islands is small. It is then possible to check the value of E_{migr} independent of E_{form} by investigating the increase in density or size of islands. It is also possible to determine at least limits on E_{form} with the appropriate experiments. These are described later.

When the flux of atoms arriving from the source is turned off, islands will grow until the mean supersaturation is eliminated. The net flux to and from each island reaches zero as the island establishes its local lateral equilibrium vapor pressure. Because of fluctuations in their initial formation and growth, there will be a size distribution of islands. The free energy of an island determines its local vapor



For

& I

ed

tion

ion/

ity Codes

l and/or

social

A-1

pressure; smaller islands will have a greater boundary free energy (more unsaturated edge bonds relative to the island perimeter), therefore be less stable, and hence have a larger lateral vapor pressure. The difference in concentrations due to differing vapor pressures at large and small islands leads to a further ordering mechanism, "coarsening" or "ripening", which is driven by the difference in boundary free energy of islands of different sizes. Figure 2 shows this process schematically. The growth (decay) rate of the large (small) islands can be written (for an assumed bimodal size distribution) as

$$r(T) \propto \nu_0 e^{-E_{\text{migr}}/kT} \left[e^{-E_{\text{form}}(1)/kT} - e^{-E_{\text{form}}(2)/kT} \right], \quad (2)$$

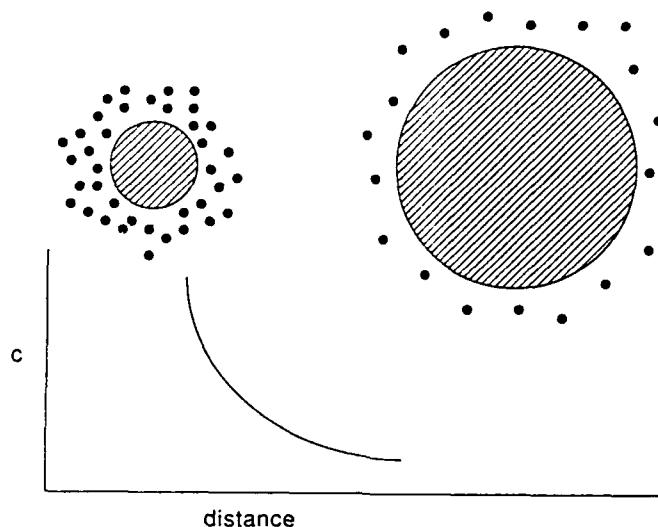


Fig. 2. Schematic diagram of the coarsening process. Small islands have a larger local vapor pressure than large islands, giving rise to a concentration gradient that drives diffusion. As the islands become similar in size, the gradient disappears and coarsening stops.

where $E_{\text{form}}(1)$ and $E_{\text{form}}(2)$ represent the desorption energies of atoms from the small and large islands respectively. The preexponential factors for desorption from large and small islands have been assumed to be the same. Equation 2 can be written as

$$r(T) \propto \nu_0 e^{-E_{\text{migr}}/kT} e^{-E_f(1)/kT} \left\{ 1 - e^{-[E_f(2) - E_f(1)]/kT} \right\}. \quad (3)$$

One can expand the last exponential:

$$\left\{ 1 - e^{-[E_f(2) - E_f(1)]/kT} \right\} = \{ 1 - 1 - \Delta E_f \}, \quad (4)$$

where $\Delta E_f = E_f(2) - E_f(1)$, and hence

$$r(T) \propto \Delta E_f \nu_0 e^{-E_{\text{migr}}/kT} e^{-E_f(1)/kT}. \quad (5)$$

The growth rate during coarsening thus always involves both a formation and a migration barrier. Therefore a pure migrational activation energy can never be obtained when desorption from islands or edges is involved. Most macroscopic measurements of diffusion (e.g., spreading of a sharp distribution) average over such effects and thus ought to generally produce an activation energy that does not represent just the activation energy for monomer self-diffusion.

The rate of coarsening also contains the term ΔE_f , which is related to the difference in island sizes. As this difference gets small, the driving force for coarsening goes to zero, and a distribution of islands all approximately the same size results (Ostwald ripening). Theoretical determinations of the asymptotic time dependence for the coarsening process⁸ for a 2D system give $t^{1/3}$. In the limit of high dilution, migration controls the rate of growth of islands, because of the large path required between islands.⁷

So far we have ignored discussion of the shape of islands, and have implicitly assumed (e.g., in Fig. 2) that they were round both during growth and at equilibrium. Islands will be round at equilibrium at any temperature if there is no anisotropy in the free energy. The free energy is

$$F = E - TS, \quad (6)$$

where E is the energy (i.e., representative of the atomic interactions in the system and any anisotropies in them) and S is the entropy. The effect of entropy is to diminish any anisotropies that exist in the mechanical energy, so that at higher temperatures generally the equilibrium shape will be smoother and less anisotropic than at OK. In systems that form distinct anisotropic structures, like the dimer rows in Si(001), it is likely that interactions are anisotropic and hence that the equilibrium island shape may be anisotropic as well, at least at sufficiently low temperatures.

In addition to an anisotropy in the equilibrium shape, there may be a growth anisotropy, given by kinetic parameters, such as the ease of accommodation of an arriving atom at an island edge with a particular orientation. The more anisotropic this accommodation is, the more anisotropic will be the growth shape. The problem can be thought of as a probability of sticking. There are several mechanisms that may be responsible for growth shapes. The most straightforward is energy accommodation of the arriving atom, in analogy with gas accommodation at surfaces. In order for an arriving monomer to stick, its energy must be transferred through inelastic collisions to the edge before it reflects and escapes the holding potential of the edge. There are numerous examples of surface-orientation-dependent gas sticking coefficients. How large an effect this can be for adsorption of atoms at different island edges is not known. Other possibilities for anisotropic accommodation are discussed below when STM data for Si(001) are considered. If the accommodation coefficient is not equal to one, Eq. (1) must be modified to include this effect. This can be accomplished by modifying the constant A , as indicated below Eq. (1).

A growth structure can clearly depend on kinetic parameters such as deposition rate (degree of supersaturation), temperature, and total coverage. At any instant, there will be competition between minimization of free energy to seek the equilibrium shape (for example by edge diffusion) and establishment of the growth shape through kinetic limitations. If the deposition rate is, e.g., very low relative to the rate at which an island can reach its equilibrium shape, the latter will

be observed. Conversely, if the deposition rate is high, a shape more related to kinetic factors will be observed.

If the flux is turned off after a growth shape is established, annealing to allow the system to coarsen also results in an island shape change. Both edge diffusion and migration between islands can affect the shape; only the latter affects island area. Differences in growth shapes and equilibrium shapes can be investigated using STM to study the coarsening process. The shapes obtained after long-time annealing represent the equilibrium shapes at that temperature; any difference between these and the initial shapes must be ascribed to kinetic factors.

No surface is truly flat. Edges of terraces separated by atomic steps can be thought of in the same context as above, i.e., as boundaries of very large islands. The structure of these edges is determined by the same rules as described above. An edge may have an equilibrium configuration or it may have a growth or evaporation shape. Anisotropy in the interaction energies may make edges with one orientation different from those with another. Anisotropy in kinetic factors can also cause different types of edges to appear different, e.g., to have different degrees of roughness or to grow (i.e., displace laterally) at different rates during deposition. In all cases, the behavior of edges and the dependence of edge roughness on temperature must be consistent with the equilibrium and kinetic behavior of islands that form during deposition.

The rest of this paper addresses in a quantitative (or at least semiquantitative) manner the issues described qualitatively above, using as an example the growth of Si on Si(001). Initial measurements for Ge growth on Si(001) are also reported.

Si(001) SURFACES

The growth of Si on Si(001) offers the opportunity to observe and explore all the processes mentioned above. The surface forms a (2x1) reconstruction, consisting of rows of dimerized surface atoms. Two reconstructions are possible, with dimer rows running along orthogonal $\langle 110 \rangle$ directions. Terraces separated by a single atomic step will have opposite reconstructions. In general, in diffraction experiments, both (2x1) and (1x2) domains are observed, a consequence of the fact that it is difficult, if not impossible, to prepare a surface that is flat (containing no steps) over an area equal to the size of the best incident probe ($\geq 10^5 \text{ \AA}^2$). Theoretical considerations⁹ of inherent strain in Si(001) predict that even a surface oriented perfectly toward [001] will break up into "up" and "down" domains, thus showing both reconstructions. There is no experimental evidence for this prediction, however, up to domain sizes $> 2000 \text{ \AA}$. Terraces this large, representing the best-aligned surfaces that have so far been available, have been observed in the STM.¹⁰

Because of the two reconstructions it is possible to create steps that have fundamentally different properties. These properties are most clearly illustrated for surfaces miscut so that the surface normal points away from (001) toward a $\langle 110 \rangle$ direction. For such vicinal surfaces, the dimer rows run alternately perpendicular and parallel to the terrace edges. As a convention, we shall call a (2x1) domain one in which the dimer rows run normal to the edges and (1x2) one in which they run parallel. The most visual evidence that these edges are energetically different¹¹ comes from STM observations of edge roughness, as shown in Fig. 3. These observations will be discussed in greater detail below. For miscuts toward $\langle 110 \rangle$, as the vicinality is increased beyond about 2° ,

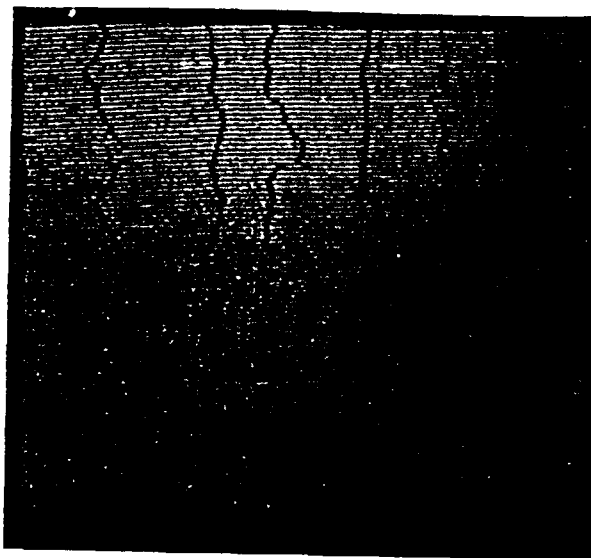


Fig. 3. STM micrograph of edge roughness in Si(001) cut toward $\langle 110 \rangle$. Edges are alternately "rough" (S_B steps) and "smooth" (S_A steps), indicating an anisotropy in the edge energies. Horizontal scale: $\sim 7,000\text{\AA}$.

double-atomic-height steps form. The nature of this transformation is not fully understood,¹² nor is the precise angle known or to what degree kinetic limitations play a role in determining the step configurations that are typically observed.^{13,14} Finally, externally applied stress affects the step configuration,^{15,16} causing one terrace to shrink at the expense of the other. The sign of the strain determines which reconstruction predominates.¹⁵

MBE of Si on Si(001) can be performed at temperatures of $\sim 500^\circ\text{C}$ with high-quality results. At room temperature and typical MBE deposition rates, several RHEED intensity oscillation cycles are observed, indicating that ordering is taking place, but that the surface quickly gets rough. Sakamoto¹⁷ has reported a number of interesting results in Si MBE. It is evident that the growth kinetics in this system are quite complex.

EXPERIMENTAL

Measurements were made in a vacuum chamber containing a STM, low-energy electron diffraction (LEED) optics, and a Si evaporator. Pressures are routinely in the 10^{-11} Torr range. The STM consists of a quadrant tube scanner mounted on a walker that allows accessing various parts of the sample. Samples are transferred from a multiple-sample "parking lot" to the STM via a manipulator. The Si surface is cleaned by a heating procedure described elsewhere.¹⁴ It leaves the surface clean with a minimum number of dimer vacancies ($< 3\%$ of surface atoms) and no other defects. Nominally flat surfaces generally had a vicinality of $\sim 0.1^\circ$, giving mean terrace sizes of $\sim 500\text{\AA}$. Recently samples oriented within $\leq 0.03^\circ$ of [001] have been used.

Depositions are performed at various substrate temperatures by evaporation from another Si wafer. The substrate temperature is measured using optical and IR fine-focus pyrometers that have been calibrated against a thermocouple for a Si sample mounted in a constant-temperature furnace. Samples are subsequently quenched to room temperature and transferred to the STM. Depositions were typically made to coverages of

a fraction of a monolayer (ML), but in some cases to as much as 10 ML.

In all of the discussions, it is assumed that the Si vapor falling on the surface consists of monomers. Mass spectrometric data for Si evaporation from polycrystalline Si "rocks" show about 10% multimers in the flux.¹⁸ It is possible that evaporation from particular surface orientations produces preferentially dimers. We are unaware that this is known. We have generally used a (111) wafer as an evaporation source.

DETERMINATION OF MIGRATION AND FORMATION ENERGIES FOR Si ON Si(001)

In the introduction we discussed the roles in growth and coarsening of E_{migr} and E_{form} , respectively the activation energies for migration and for lateral desorption of a diffusible Si entity (here assumed to be a Si monomer), from an edge. One can separate these and (at least in principle) determine them quantitatively using STM.

A lower limit to E_{form} can be obtained simply from STM observations of possible fluctuations in the structure of terrace or island edges. Atoms desorbing from an edge and readsorbing somewhere else on the edge change the edge structure over time. If no changes occur in the structure, one can put a lower limit on E_{form} . The rate of lateral desorption from an edge is given again by

$$r(T) \propto \nu_0 e^{-E_{\text{form}}/kT} \quad (7)$$

Terrace edges in Si(001) of both kinds shown in Fig. 3 are stable even locally over a period of at least hours at room temperature. Using $\nu_0 = 10^{12}/\text{sec}$ gives a limit for $E_{\text{form}} > 0.8$ eV/atom (compare to the cohesive energy of Si, $E_{\text{coh}} = 4.64$ eV/atom). Any value smaller than this would result in observable differences in edge structure over a period of one hour. Its magnitude suggests that it is quite difficult to remove an atom from either type of edge. The desorption barrier is not the same quantity as the relative energy of a step, as calculated, e.g., by Chadi.^{11a} Chadi calculates the difference in energy between a flat surface and one containing a step, per unit length of edge. This number may be small while the desorption energy is large. The value of $\nu_0 = 10^{12}/\text{sec}$ is the standard estimate of attempt frequency. It may be smaller, but in order to reduce E_{form} significantly, its value would have to be unreasonably small.

One further conclusion of the stability of edges is that migration along the edge is also negligible at room temperature. One expects that a lower barrier would in general need to be overcome for edge diffusion than for lateral desorption. Hence the above limit more properly refers to edge diffusion, with desorption energies probably even larger. It should be noted that the above result gives no conclusion about the nature of the species that desorb or diffuse along the edge when the kinetics do become significant. It is possible that this unit is a dimer at least in some situations.

A large value of E_{form} confirms our previous assumption that the influence of the lateral desorption term is negligible in growth of Si on Si(001) even at relatively low supersaturations and high temperatures. One can therefore determine E_{migr} in an experiment that measures the surface self-diffusion coefficient. A physical picture of this procedure can be obtained by considering a bare terrace bounded by steps, one "up" and one "down", to which one atom is added from the 3D gas phase. This atom will diffuse on the surface until it finds the step. The parameter important here is the diffusion coefficient of the monomer and its

activation energy. If more than one atom arrives, they may meet each other before finding the step. The chance then exists to form an island, which will subsequently grow as other monomers strike it. If the edges of the terrace are far away, essentially all the monomers will form islands. Initially, almost all monomers stick to each other and form new islands, leading to an early rate of increase of the number of islands proportional to t^3 . As the number of stable islands increases, this rate decreases because monomers will have a probability of finding existing islands instead of other monomers. The surface diffusion coefficient determines how large an area a monomer can interrogate in a given time, and thus determines the probability of a monomer finding an existing island before a new monomer is deposited in its vicinity (for a given deposition rate R). Therefore the surface diffusion coefficient ultimately determines the number density of stable islands after deposition to a certain dose with a given rate R . Thus simply by counting the number of stable nuclei that have formed in a known substrate area at a particular substrate temperature, one can estimate the diffusion coefficient at that temperature.^{5,19} Thus the island density will reflect the deposition rate as well as the substrate temperature (changing D). The activation energy for diffusion can be extracted from measurements at different temperatures.

Figure 4 shows STM micrographs of the distribution of Si islands after deposition to four doses at a fixed rate and a substrate temperature of 475K. Similar measurements have been made down to room temperature.¹⁹ From them several conclusions are possible: 1) Islands form at room temperature, implying diffusion is occurring at room temperature. The islands are of monolayer height, and the stable nucleus appears to be one dimer. 2) The density of islands increases with increasing dose, initially rather rapidly and then more slowly. Islands also grow. 3) Islands have anisotropic shapes; this anisotropy is more pronounced at higher growth temperatures. 4) For fixed dose there are fewer islands for deposition at higher temperatures than at lower. 5) Although defects occur in the substrate, there is not a pronounced decoration effect, i.e., defects do not play the decisive role in determining the density of islands that form. 6) Once the flux is off, the island distribution is invariant at room temperature; a measurable rate of island coarsening takes place only for annealing temperatures above about 520K. This fact is important because it implies that the images in Fig. 4 represent effectively the island configuration at the end of deposition. The last observation confirms the result that E_{form} is large.

Figure 5 shows a plot of the stable-nucleus density as a function of dose at otherwise identical conditions but at two substrate temperatures. As expected from the above qualitative argument, the higher diffusion coefficient at higher temperatures should produce a lower stable-nucleus density. Fits to these data with a rate equation model of surface diffusion²⁰ that takes into account island nucleation, loss of monomers to edges, and adsorption of monomers at existing islands are shown in Fig. 5. From these fits we extract diffusion coefficients of roughly 1×10^{-12} cm²/sec and 2×10^{-12} cm²/sec respectively at 300 and 475K. The model gives the rate of change with dose (time) of the number of monomers (diffusible species) $n(x,t)$ in terms of monomer gain and loss terms:

$$\frac{\partial n(x,t)}{\partial t} = R + D \nabla^2 n(x,t) - D n^2(x,t) - D^2 n(x,t) \int_0^t dt' n(x,t')^2, \quad (8)$$

where R is the deposition rate and D is the surface self-diffusion coefficient. The integral over time of $D n^2(x,t)$ represents the total number density of islands. Edges bounding a terrace of finite size and

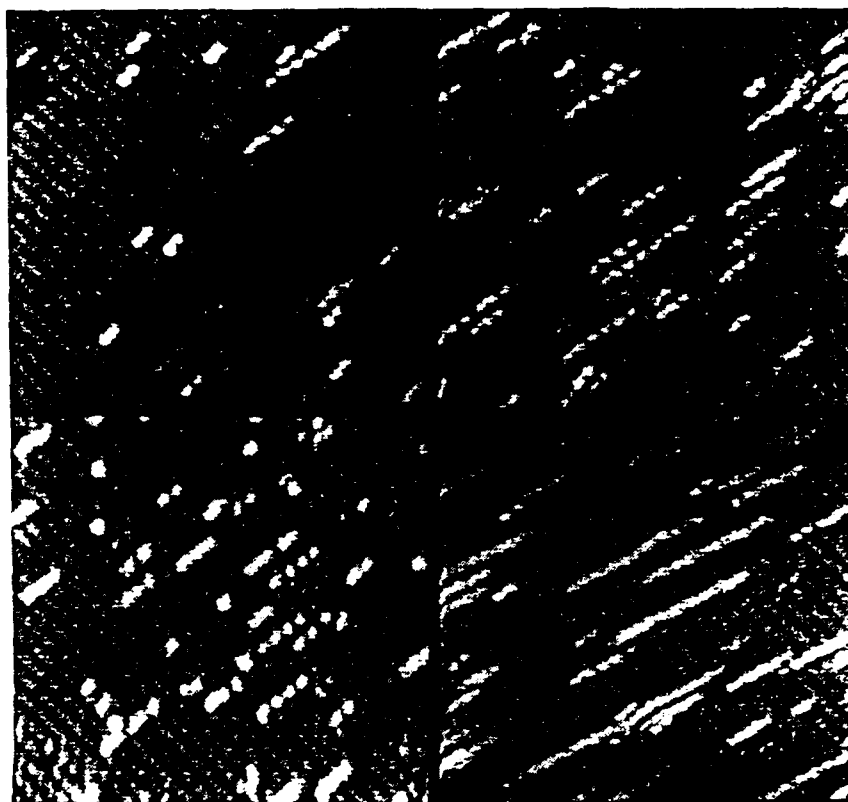


Fig. 4. STM micrographs of the distribution of Si islands after deposition to four doses at a fixed rate and substrate temperature $T = 475\text{K}$. Islands show a considerable shape anisotropy. Each panel is $230\text{\AA} \times 230\text{\AA}$. Left to right, top: 0.05, 0.1 ML; bottom: 0.15, 0.2 ML.

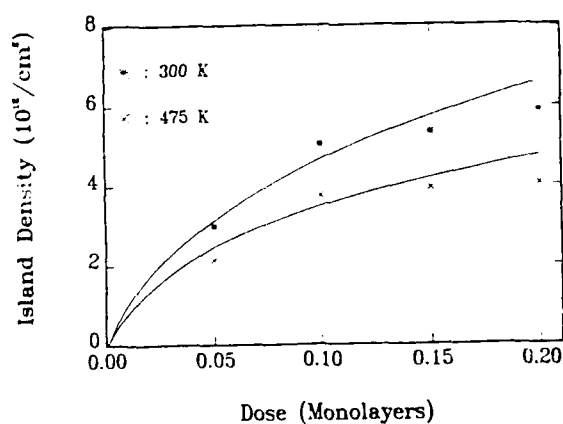


Fig. 5. Determination of diffusion coefficients of Si in Si(001). The number density of stable nuclei is plotted vs dose at two temperatures. The fit is from Eq. (8).

acting as sinks can be introduced in the boundary conditions. For sufficiently large terraces and low temperatures (short diffusion lengths) the loss to edges is negligible. Island coalescence is not considered here. The model is applicable only at low doses.

The values of D at the two different temperatures are not greatly different. In view of the large uncertainties, these differences may not be significant. Nevertheless, if we are permitted to assume that they are, and that two points determine a line, we can extract an (at this stage very rough) activation energy for diffusion. The value is 0.04 eV/atom. This is a very small value based on usual concepts of activation energy for surface diffusion. A simple calculation illustrates this. Using the conventional value for the attempt frequency $\nu_0 = 10^{12}$ /sec, a value of $D \approx 10^{-12}$ cm²/sec requires an activation of energy of the order of $E_{\text{migr}} = 0.5$ eV if thermal activation is limiting the rate of diffusion. Alternatively, $E_{\text{migr}} \sim 0.04$ eV requires $\nu_0 \sim 10^2$ - 10^3 . If this small experimental value for E_{migr} proves to be correct, it suggests one of at least two possibilities: 1) The activation energy for diffusion of Si on Si is a small fraction of the energy required to break bonds and reform them,⁶ i.e., there is a minimum-energy path, as for cleavage^{6b} that is much lower than one might expect from a simple bond-breaking argument. This possibility does not address the problem of the very small prefactor that would then be required. 2) Diffusion in this temperature range is not determined by thermal activation but rather by the heat of condensation and accommodation of the arriving Si species. This possibility can be pictured as follows. To accommodate and come to rest, an incoming atom has to lose its heat of condensation. The atom will have a diffusional range that depends on how well this energy is transferred to the lattice. If the heat of condensation is controlling the diffusion, there should be no temperature dependence to the diffusion coefficient. Eventually at higher temperatures the thermal activation must begin to dominate and one would expect to see a knee in the Arrhenius relation between $\ln D$ and $1/T$.

A second way to determine diffusion coefficients on surfaces rests on the same principle of an interrogated area, but uses the edges of terraces as sinks, in competition with stable nuclei. The consequence should be a denuded zone near terrace edges, i.e., a mean capture distance associated with an edge in which the nucleated-island density is much smaller. If the edge is assumed to be a perfect sink, a simple analysis²¹ gives directly the diffusion coefficient. An STM micrograph demonstrating the effect is shown in Fig. 6. The micrograph suggests several interesting extensions and also complications. If the edge is not a perfect sink, (see also below), the diffusion coefficient is underestimated. Different types of edges may have different accommodation coefficients and hence show different denuded zones. The accommodation of atoms arriving at the edge from the upper terrace and from the lower terrace may be different, giving different denuded-zone widths for the same diffusion coefficient. Finally, the diffusion coefficient may itself be anisotropic, producing different denuded-zone widths in different directions even if the accommodation is the same. The different aspects of the problem can be sorted out by the appropriate experiments,²¹ as discussed briefly below.

ANISOTROPIC ISLAND SHAPES: GROWTH OR EQUILIBRIUM STRUCTURES

In the introduction we differentiated between growth shapes, dependent on kinetic factors, and equilibrium shapes, controlled by the free energy of the structure. Figure 4 showed a considerable anisotropy

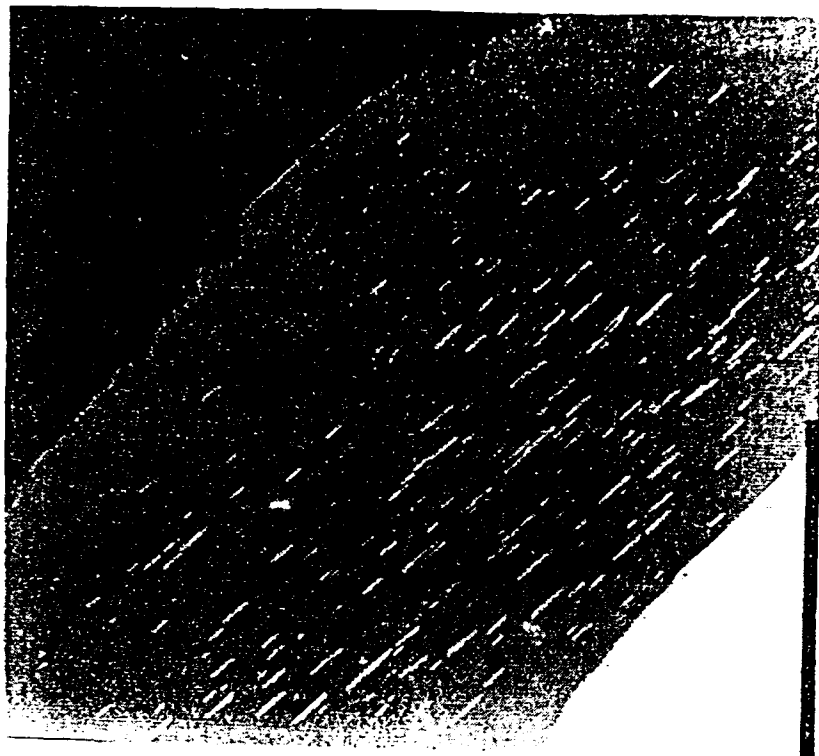


Fig. 6. STM micrograph of Si growth on nearly perfectly oriented ($\leq 0.03^\circ$ misoriented) Si(001) at 540K, showing denuded zones free of islands near certain terrace edges. This sample was strained so that the majority domain terraces become very large, while the minority domains shrink to $< 300\text{\AA}$ and to near zero in some spots. Five levels are shown. The denuded zone implies that migration downwards over the rough edge is highly likely and thus does not see a large barrier. The lack of a significant denuded zone at the smooth ("up") edge (lower right) further confirms that atoms do not stick very well on this edge. (Dose: ~ 0.1 ML. Scale $1 \times 1 \mu\text{m}$).

in island shape, observed as well by others.^{22,23} Coarsening experiments can differentiate between growth and equilibrium shapes, as the islands approach this equilibrium configuration during annealing. Figures 7 and 8 show examples of the consequence of annealing. In all cases we have found a shape change toward lesser anisotropy.²⁴ Generally we observe, after annealing, aspect ratios of about 2 and certainly less than 3. Even anneals at $T > 800\text{K}$ produce about the same anisotropy. We can not conclude from Figs. 7 and 8 that the shapes shown there are at equilibrium. Because of the limited terrace sizes in the substrates to which we have access there is continued loss of atoms to edges and further annealing will eventually lead to terraces free of islands. Therefore true equilibrium can not be reached if any information on islands is desired; however, all of our measurements suggest that true equilibrium would be in the direction of rounder islands. This conclusion affects shapes from higher-temperature anneals more than those from lower temperature anneals. We conclude that the boundary free-energy anisotropy in Si(001) in orthogonal directions is $\sim 2:1$ for $T \approx 600\text{K}$, a temperature at which coarsening and boundary migration are sufficiently rapid to allow us to observe shape and size changes, and does not change drastically at higher temperatures. Because we do not observe significant kinetics below 500K in laboratory times, we can draw



Fig. 7 STM micrographs of the distribution, shape, and size of Si islands after annealing at $\sim 625\text{K}$. The initial dose is about 0.2 ML. By annealing, some adatoms merge into substrate steps. Scale $1000 \times 700 \text{\AA}$.

no concrete conclusions about the equilibrium anisotropy at room temperature, except to suggest its direction: it will be slightly larger than at higher temperatures. Entropy tends to equalize the boundary free energies in different directions. The mechanical energy contribution to the boundary free energy is positive and can be thought of as the interaction energy stored in the unsaturated bonds at the edge. Assume now that bonds are strong in one direction and weak in the orthogonal one. In the direction in which the broken bonds are weak, the mechanical energy is a small positive number; the corresponding boundary free energy in that direction will be smaller than in the orthogonal one, in which the mechanical energy is high. It should be noted that it is expensive to create a kink on the low-energy edges (high kink excitation energy), because that kink will have a segment of the high-energy step. Conversely, kinks are easily created on the high-energy edges, because it costs very little mechanical energy to create them. This is why the high-energy edges of islands or terraces are "rougher". A schematic boundary free-energy anisotropy plot²⁵ is shown in Fig. 9. As the temperature is increased, entropy reduces the free energy in all directions, but by different amounts. This occurs because entropy is itself a function of the temperature and the strength of the interactions and hence different in different directions. The entropy is given by

$$S = k \left[\ln Z - \beta \frac{\partial \ln Z}{\partial \beta} \right], \quad (9)$$

where

$$Z = \sum_n e^{-\beta E_n}, \quad \beta = 1/k T$$

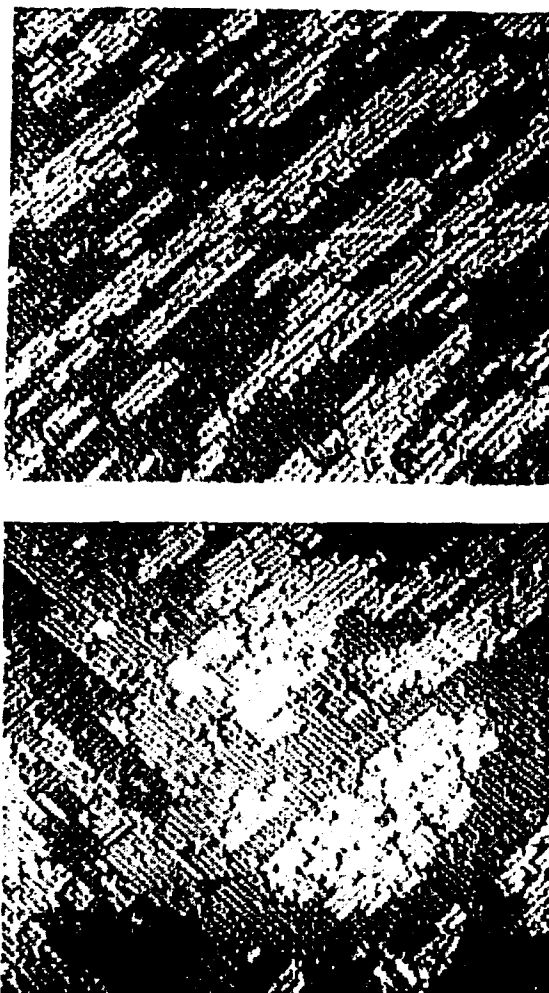


Fig. 8 STM micrographs of Si islands on Si(001). Top: grown at 575K at 1/20 ML/sec, coverage ~ 0.5 ML; bottom: after annealing at 575K for 10 min. Scale is $500\text{\AA} \times 500\text{\AA}$.

and E_n is the mechanical energy of a configuration and the sum is over all configurations. The free energy of edges on which the kink excitation energy is small will be reduced more by an increase in temperature than that of the stable edges, on which the kink excitation energy is large. Consequently islands become rounder at higher temperatures. This argument implies that the anisotropy in the mechanical energy (equal to the free energy at 0K, or the unsaturated bond strengths) will be larger than the $\sim 2:1$ ratio of free energies at 500K determined in the experiments. We have made calculations,²⁰ based on a 2:1 free-energy ratio at 500K, the apparent weak temperature dependence of this ratio, and estimates of the correlation lengths of the roughness of S_A and S_B steps that suggest kink excitation energies of ~ 0.08 eV and 0.2 eV/atom for the S_A and S_B steps in Si(001) respectively. Because the smallest observable kinks in both directions consist of two dimers, the corresponding mechanical energies are half of these values, or 0.04 eV and 0.10 eV/atom. These should be compared with the values of 0.01 eV and 0.15 eV/atom determined by Chadi.^{11a} Figure 10 shows quantitatively what we stated qualitatively above, that the free energy of the high-energy (S_B) edge is much more dependent on temperature than

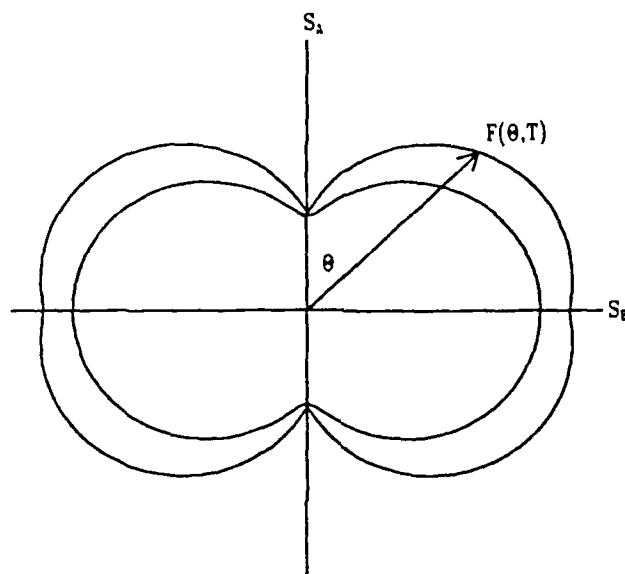


Fig. 9 Schematic polar plot of the boundary free energy of 2D islands with anisotropic interactions, given in text, at two temperatures. At higher temperature, entropy reduces the free energy, but by different amounts in different directions. The equilibrium island shape is obtained in the standard manner²⁵.

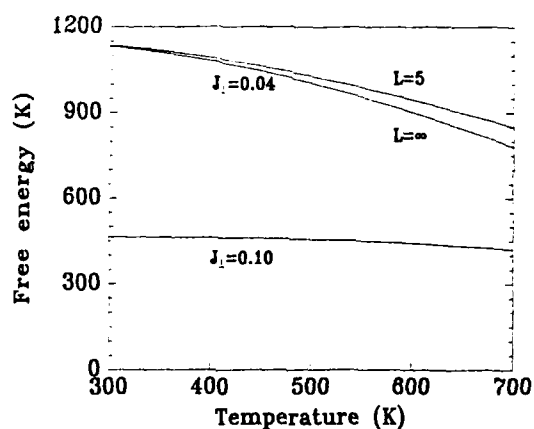


Fig. 10. Calculation of the temperature dependence of the free energy for S_A and S_B steps in Si. Values of 0.04 and 0.1 eV/atom are used for the edge energies. Excitation energies used in the calculation are twice this large because we observe chiefly double-dimer kinks. Also shown is the free energy for the S_B edge for an island constrained to a width of five dimer rows.

the low-energy (S_A) edge. To the extent that the two free-energy curves converge, the island shape anisotropy should be temperature dependent. We do not observe a significant effect of this sort, although we can only make measurements over a limited temperature range. The free-energy curves can be flattened by shifting them both upward in mechanical energy, making it more costly to create kinks. For small islands, there is another factor that needs to be considered, namely that, for a limited line length, fewer configurations are possible and the partition function in Eq. (9) should be summed over only a finite range. Hence the entropy contribution should be less important for small islands. A calculation for the S_B edge of an island with a width of five dimer rows is also shown in Fig. 10. It can be seen that the dependence of the free energy on temperature is somewhat weaker. For smaller islands, the effect of entropy is even weaker; for a single line of atoms, the free energy reflects just the mechanical energies. The islands on which we have measured anisotropy range from four or five dimer rows wide up to 50 or more. In all, the anisotropy is of the order of 2 or 3. This result suggests that the mechanical energies must be high to begin with, so that entropy is not extremely important in controlling the shapes. The values of .04 eV/atom and 0.1 eV/atom that we suggest above for the S_A and S_B edge energies are the consequence of this reasoning.

The observed anisotropy during growth is as large as 15-25 at temperatures at which the equilibrium shape anisotropy is $\sim 2:1$. This is shown in Fig. 11 and also in Fig. 4. Hence a kinetic limitation must be present. In the limit of high deposition rates and temperatures low compared to coarsening temperatures, the kinetic process dominates and the island shape anisotropy reflects essentially the accommodation coefficient anisotropy at the sides and ends of dimer rows. We conclude that this anisotropy may be as much as a factor of 10 or more.²⁴ We have already mentioned in the introduction the most generally quoted cause for an accommodation coefficient differing from one, namely the ease of transfer of the arriving atom's energy to the stable structure. Such transfer probabilities may differ for different edges, much as they do at surfaces with different orientations. It may be difficult to justify a factor of ten in this manner, however. A more likely explanation is that an arriving monomer can bond more easily and directly on the end of a dimer row than at a side. Attachment at a side would be equivalent to the incipient formation of a new row, and probably requires a dimer, not just a monomer. A monomer then would have a very short residence time on the side (very low binding energy). On the end the picture is different. Here the substrate bond configuration is such that it should be easy for an atom to attach. In fact, the bonding arrangement of Si atoms in the substrate requires that there are two types of bonding sites for an arriving atom at the end of an existing dimer row, one right at the end, and the other displaced by one row lattice constant. We refer to the latter as the "diluted-dimer" structure.¹⁹ We have observed that the latter frequently occurs during the early stages of growth,¹⁹ suggesting that it is a slightly more favorable site for initial binding than the "close-packed-row site". Figure 11 shows examples of the diluted-dimer structures. If, as mentioned earlier, the diffusing species is a dimer and not a monomer, the above arguments on accommodation transfer straightforwardly. It would be energetically more favorable as well for a dimer to attach at the end of a dimer row than to attempt to form a new row.

To summarize, equilibrium island shapes in Si at $T \sim 500K$ have a maximum aspect ratio of $< 3:1$, implying that the boundary free energies in orthogonal directions (normal and parallel to dimer rows) differ by no more than this factor. Because entropy reduces the island shape

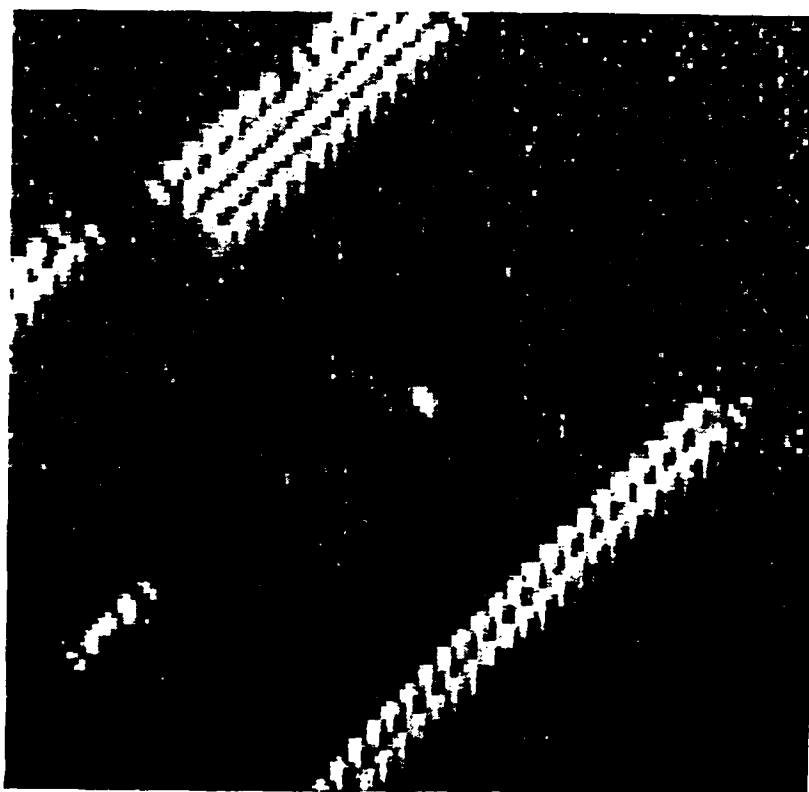
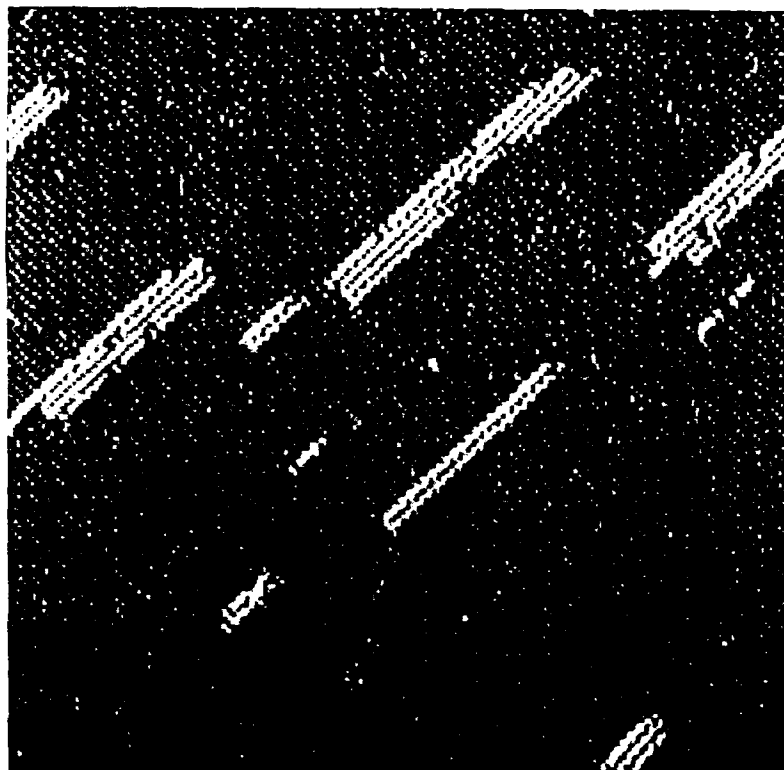


Fig. 11. STM micrographs of growth structures of Si on Si(001) at high resolution; top 600Å x 600Å, bottom: 250Å x 250Å. Islands are quite anisotropic. At the ends of many rows, one can observe the "diluted-dimer" structure, in which a dimer is missing between the end of the completed row and the final adsorbed dimer. This is particularly evident in the leftmost two islands in the lower micrograph. A single dimer is also observable in the center of this micrograph.

anisotropy, the interaction energies can be more anisotropic; preliminary calculations suggest an anisotropy of $\sim 2.5:1$ in kink excitation energies and values of ~ 0.04 eV and 0.1 eV/atom for the edge energies of type S_A and S_B steps respectively. Because the equilibrium shapes are only mildly anisotropic most of the shape anisotropy observed during growth must be a kinetic phenomenon. We have suggested accommodation coefficient models to explain the anisotropy, with an anisotropy in this coefficient of $\geq 10:1$.

Similar results are observed for submonolayer Ge deposited on Si(001).²¹ Equilibrium islands with a (2×1) structure (dimer rows) form. Growth and equilibrium shapes are shown in Fig. 12. The mechanisms for

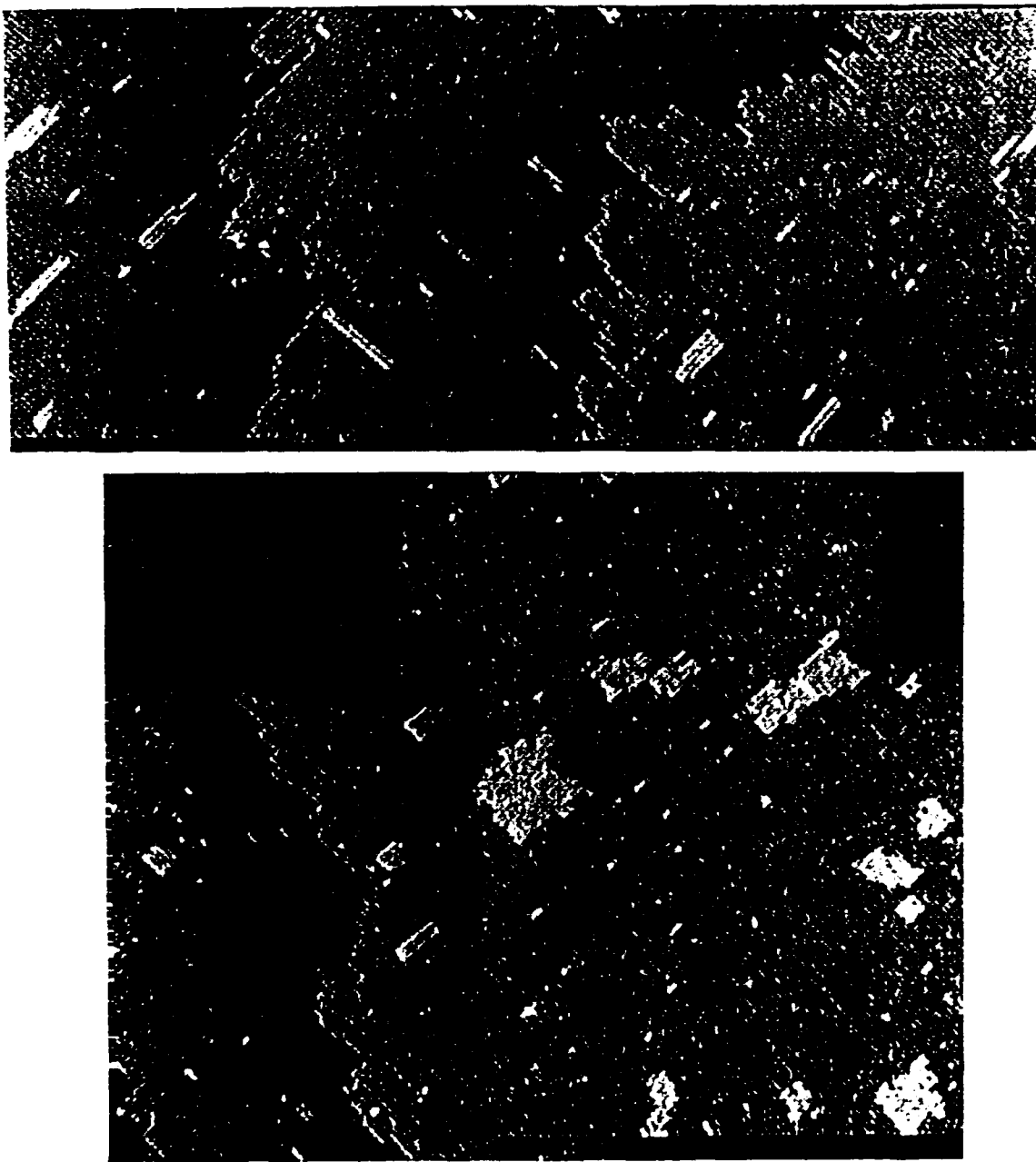


Fig. 12 STM micrographs of 2D Ge islands on Si(001) top: deposited at 500K, ~ 0.05 ML, $R = 1$ ML/40 min., scale: $1500 \times 600 \text{ \AA}$. Islands are oblong as for Si bottom: annealed at 575K for 10 min., scale: $1400 \times 1150 \text{ \AA}$. Islands are nearly equiaxed.

Si and Ge growth and ordering appear to be quite similar. For growth at sufficiently high temperature, Ge accommodates at steps in the Si substrate, creating bands of Ge that follow the Si edges. This conclusion is obvious from topographic pictures, although we have not directly observed electronic difference across the junction area. By comparing Si and Ge growth at similar coverages, rates, and substrate temperatures, one can, in principle, obtain a comparison of their migration and formation energies and the relative degree of anisotropy in their accommodation at different edge types during growth.

TERRACE EDGES: EQUILIBRIUM STRUCTURES AND GROWTH SHAPES

Terraces are simply large islands. The behavior of terrace edges, in particular their roughness and the behavior during growth, must follow the same thermodynamic and kinetic laws as smaller islands, with the assumption, already discussed, that size effects are absent. As described above, for the proper vicinal miscut (toward $\langle 110 \rangle$) the two types of edges correspond to island edges with dimer rows parallel and perpendicular to the edge. The dimer row orientation for which the "down" step is rough is also the one for which the island edge is ragged. Edge roughness must be explained on the same basis and be consistent with islands shapes. At any temperature, the edge free energies guide the degree of roughness. To agree with the island shape anisotropy they can differ by no more than a factor of ~ 2 at 600K, which must suffice to explain the difference in edge roughness of the two types of edges in Si(001) cut toward $\langle 110 \rangle$. (This statement assumes no island size effects in the free energy). In a direction that produces a rough edge, the total "line length" of strong bonds can be maintained while inserting kinks of the other edge type that cost only a small mechanical energy. By doing so a reduction in free energy is achieved through the larger increase in entropy resulting from using a larger region of phase space (more possible configurations of edge atoms). Interaction energy ratios can be higher than 2:1, as described, because the entropy reduces this anisotropy. At any finite temperature, the free energy determines the configuration, however. We are attempting to determine the correlation lengths of edge roughness directly from STM micrographs. For the terrace edges we do not know as well as we do for the islands the temperature for which the configuration shown in the micrographs is the equilibrium one. Clearly it is not the equilibrium configuration for any temperature below ~ 500 K, at which we first observe sufficient kinetics for coarsening to occur. It is possible that the cooling rate causes some "freezeout" to occur already at higher temperatures. We estimate that the configuration shown, e.g., in Fig. 3, represents equilibrium at a temperature between 500 and 600 K. Experiments are in progress using LEED to measure the edge roughness directly at various temperatures by analyzing the diffracted-beam profile in the appropriate direction.²⁶ Calculations have been performed to show that diffracted-beam profiles can be quantitatively related to the correlation function of edge roughness and that from the latter, edge energies can be deduced.²⁷ With such information, it will be possible to extract the entropy contribution to edge roughness and the absolute ratio of interaction energies at the two steps, and to establish consistency with the equilibrium island shapes.

Edge roughness and atomic configuration are affected by other factors, notably by strain due to externally applied stress and by degree of vicinality. In both cases, one can think of a constraint on the roughness due to the constraint of terrace size. Strain causes one type of terrace to grow at the expense of the other.¹⁵ Increased vicinality makes all of them small. Not all configurations are possible when

terraces are small, causing terrace edges eventually to become straighter. Figure 13 shows a micrograph for a 4° miscut surface. The edges are quite straight. A direct comparison with Fig. 3 is not possible, of course, because a 4° vicinal surface has double-height steps. However, samples stressed in such a manner that the (1x2) terrace is small do appear to give less local roughness in the S_B terrace edges than do unstrained samples. The kinetics of step motion in a strained surface is discussed elsewhere in this volume.²⁸

During deposition, edges may develop growth shapes in the same manner as islands. In particular, for vicinal surfaces cut toward $\langle 110 \rangle$, edges that have dimer rows normal to them grow at a faster rate than do those with dimer rows parallel, catching up to the latter to form double-height steps after deposition of $\sim 1/2$ ML. This phenomenon has been observed both by RHEED¹⁷ and by STM.²³ The boundary free-energy differences between the two edges at typical growth temperatures can not differ by more than a factor of ~ 2 . Any effect beyond this must again be ascribed to anisotropic accommodation at the different edges. We believe that such anisotropic accommodation is one of the fundamental aspects of growth in materials like Si, Ge, and possibly also GaAs.

DIFFUSIONAL ANISOTROPY AND GROWTH

We have shown that anisotropies in boundary free energy, in energy, and in accommodation occur in Si-on-Si(001) ordering and growth and suggest that they can occur in general in materials that have anisotropic surface structure. Additionally in Si the intrinsic surface stress is anisotropic.^{9,15,28} It would not be surprising if the surface diffusion coefficient were also anisotropic. Such an anisotropy is difficult to verify because of the existence of some of the other effects described above.

The simplest way to check diffusional anisotropy would be to search for differences in denuded zones (such as those shown in Fig. 6) on terraces with edges aligned parallel and orthogonal to the expected direction of rapid diffusion. In the direction of rapid diffusion, a larger denuded zone should be observed. In Si(001), one might expect physically the direction of rapid diffusion to be along dimer rows, and the slow direction across dimer rows (although the opposite has also been suggested). For this form of diffusional anisotropy, a miscut toward $\langle 110 \rangle$ assures the correct geometry, producing alternate terraces that look identical with respect to diffusion behavior. For Si(001) miscut by more than 2° , all terraces have dimer rows running perpendicular to the edges, and it becomes impossible to study diffusional anisotropy. In other materials, such as GaAs(001), which forms double-layer steps, it is necessary to produce vicinal surfaces with different terminations, which then have the crystallographic axes in one case parallel and in the other perpendicular to the steps, with all terraces of a given termination being identical. In any case a determination of the diffusion coefficient from the denuded zone gives too low a value for D if one assumes perfect sticking, but the accommodation coefficient is actually less than one.

If the edges are equivalent in their ability to capture the diffusing species, then a larger denuded zone will form near those edges for which the rapid-diffusion direction is normal to the edges. If, additionally, the capture probability of a "down" step is the same as that of an "up" step, the denuded zone on each terrace will be symmetric (although different on alternating terraces in vicinal Si(001)). Neither of these conditions is assured. We have already demonstrated that the

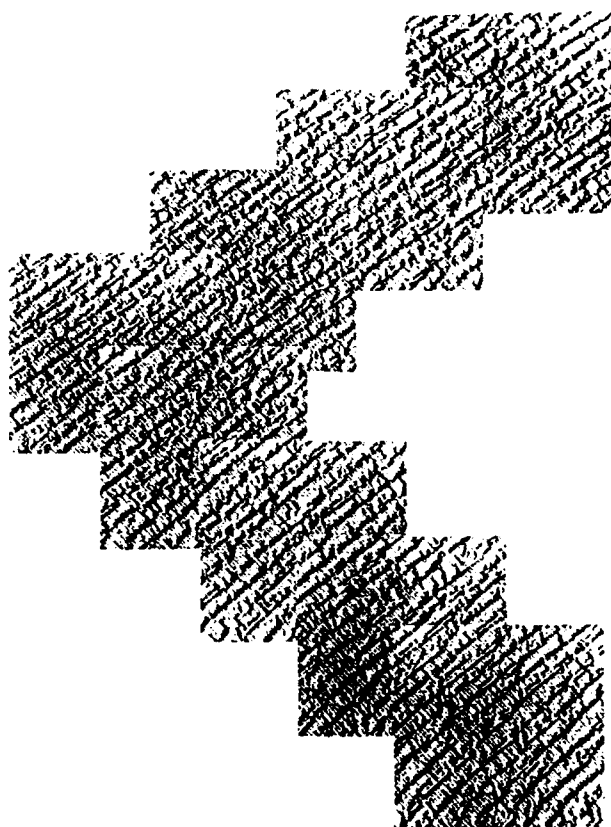


Fig. 13 STM micrograph of vicinal Si(001) cut 4° toward $\langle 110 \rangle$. The surface has double-height steps. Scale: $\sim 2000\text{\AA}$ along each diagonal. Compare with Fig. 3.

accommodation coefficient at S_B and S_A edges is different. Hence the denuded zones can not be symmetric on any terrace for Si(001) cut toward $\langle 110 \rangle$ because each terrace is bounded by an S_A and an S_B edge. We can, however, definitively show that the capture at an S_B "down" step is as great as an S_B "up" step,²¹ implying that there is no (or at most a very small) barrier to mass transport "downstairs". Mass transport "downstairs" is an essential ingredient for epitaxial growth, because lower levels must be preferentially filled to obtain layer-by-layer growth. It is frequently assumed in MBE modeling, however, that the downward flow is small and that most atoms deposited on a terrace migrate to and adsorb on the "up" edge.

The information that accommodation is similar, (if not the same) on an S_B edge for atoms arriving from above and below the edge can be used to determine the anisotropy in diffusion coefficient, because on the "up" terrace the dimer rows are normal to the edge, while on the "down" terrace they are parallel. From observations of this sort, we determine qualitatively a faster diffusion (near room temperature) along dimer rows. The same measurement is in principle possible at S_A edges, except that the accommodation at these edges is so small that at any reasonable temperatures and coverages the denuded zones are too small to make a clear differentiation between them. An absolute value of D can not be obtained in this manner unless one assumes the accommodation coefficient equal to one. This is probably a good assumption for S_B steps over a wide temperature range. One may also be able to separate the diffusion coefficient if it and the accommodation coefficient have different

temperature dependences.²⁹ One may expect that the accommodation coefficient, if it is an electronic effect as we suggest, has only a weak temperature dependence. Then from the temperature dependence of the denuded zones, the activation energy and preexponential factor of D can be obtained. Such measurements are in progress.

If diffusional anisotropy exists, can it affect island shapes during growth? We have addressed this question using Monte Carlo calculations and have concluded that it can not.²⁴ This conclusion can also be reached on physical grounds, by considering the availability and arrival of atoms at an island in a 2D lattice. Hence the growth shapes of islands and the observation of double-height layer formation during Si epitaxy^{17,23} are likely not a consequence of any possible anisotropy in diffusion.

SUMMARY AND CONCLUSIONS

We have provided a brief overview of mechanisms operative in the ordering and growth of two-dimensional layers and have illustrated those with STM measurements for the submonolayer growth of Si and Ge on Si(001). Several classical concepts in the thermodynamics and kinetics of growth can be observed in these 2D systems, and in some cases quantified. The concepts considered include self-diffusion on surfaces, thermodynamics of island shapes and sizes, and kinetics of growth and coarsening, including accommodation.

In the diffusion measurements, we distinguish in the activation energy for diffusion between a migration term and an energy for formation of a diffusible species (an energy for desorption from an edge). We show that the latter must be large ($\geq 0.8\text{eV}$) for Si on Si(001). We demonstrate the appropriate measurements and theoretical evaluation to determine a surface self-diffusion coefficient based purely on migration. We obtain a value of $\sim 10^{-12} \text{ cm}^2/\text{sec}$ at room temperature for Si on Si(001), sufficient to cause ordering to occur. One might offhand conclude that this result would predict that MBE of Si on Si(001) is possible at room temperature. In fact, several RHEED oscillations, indicating islanding for several layers before the surface becomes uniformly rough, are observed.³⁰ However, good growth at room temperature is not possible because other processes, including migration over edges and desorption from existing islands are part of the total epitaxial growth process. Desorption from edges appears, at least to be a slow process.

In experiments in which Si is deposited onto the surface for $T < 500^\circ\text{K}$, our measurements suggest that the effective activation energy for migration is very small. We speculate that we may be observing a heat-of-condensation effect, in which the diffusion is no longer purely controlled by thermal activation through the substrate, but rather by the efficiency with which the heat of condensation of the incoming species is given to the lattice.

We have shown, through coarsening experiments, that the free-energy anisotropy of Si islands on Si(001) can be no more than $\sim 2:1$ at $T > 500\text{K}$. Fitting island shapes to a model calculation of the boundary free energy suggests values for the step energies of 0.04 and 0.10 eV/atom respectively for S_A and S_B steps.

We observe, during growth, an island shape anisotropy more like 15:1 or greater. This large anisotropy must be a kinetic effect, i.e., an accommodation coefficient anisotropy. We suggest a qualitative model that invokes the difference in ability of monomers to bind at the ends

and sides of existing dimer chains. We suggest that these probabilities of accommodation differs by a factor of ten. We do not know the absolute values of accommodation at either edge.

Any time accommodation less than one exists at an edge, a measurement of the diffusion coefficient that depends on a denuded zone or the absence of islands in the terrace (e.g., RHEED intensity oscillation damping at high growth temperatures in GaAs) will give an answer that is too low. A factor of ten decrease in accommodation will lead to a factor of 10 increase in the measured value of D . In different terminations of vicinal GaAs(001) surfaces, the terrace edges are different,²⁶ and it is quite possible that the accommodation coefficient is as well. An accommodation coefficient whose magnitude depends on the nature of the edge would give different measured values for D on the two types of terraces, even if it actually were the same.^{26c} Anisotropic accommodation can affect our measurement of diffusion just as they can the RHEED measurements above if accommodation is less than one at the ends of dimer chains. The ideal situation for the model is that the accommodation coefficient equals 1 at the ends of dimer chains (S_B steps) and 0 on the sides (S_A steps). This result is approximately correct, since there is an observed factor of >10 difference in its value on the sides and ends. We expect our determination of D to be, therefore, only weakly affected by the anisotropy in the accommodation coefficient, and to be relatively accurate.

Acknowledgements

This research has been supported by the U.S. Office of Naval Research and in part by the U.S. National Science Foundation, Grant No. DMR 86-15089. We thank Dr. P. Wagner, Wacker Chemitronic, Burghausen, Germany for supplying us with high-quality, well oriented Si wafers for part of this work.

REFERENCES

1. Epitaxial Growth, J. D. Matthews ed., Academic, New York (1975).
2. B. Lewis and J. C. Anderson, Nucleation and Growth of Thin Films, Academic, New York, (1978).
3. W. K. Burton, N. Cabrera, and F. C. Frank, Phil. Trans. Roy. Soc. (London) A243, 299 (1951).
4. E. Bauer, Z. f. Kristall. 110, 372 (1958).
5. J. A. Venables, G. D. T. Spiller, and M. Hanbücken, Rept. Prog. Phys. 47, 399 (1984).
6. a) P. J. Feibelman, private communication.
b) J. E. Northrup and M. L. Cohen, Phys. Rev. Letters 49, 1349 (1982).
7. M. Zinke-Allmang, L. C. Feldman, and S. Nakahara, this volume.
8. a) I. M. Lifshitz and V. V. Slyozov, J. Phys. Chem. Sol. 19, 35 (1961).
b) D. A. Huse, Phys. Rev. B34, 7845 (1986).
9. O. L. Alerhand, D. Vanderbilt, R. Meade, and J. Joannopoulos, Phys. Rev. Letters 61, 1973 (1988); V. I. Marchenko, Pis'ma Zh. Eksp. Teor. Fiz. 33, 381 (1988) [JETP Lett. 33, 381 (1988)].
10. Y.-W. Mo and B. S. Swartzentruber, unpublished.
11. a) J. D. Chadi, Phys. Rev. Letters 59, 1691 (1987).
b) D. E. Aspnes and J. Ihm, Phys. Rev. Letters 57, 3054 (1986).
12. O. L. Alerhand, A. N. Berker, J. D. Joannopoulos, D. Vanderbilt, R. Hamers, and J. E. Demuth, Phys. Rev. Letters 64, 2409 (1990).
13. C. E. Aumann, D. E. Savage, R. Kariotis, and M. G. Lagally, J. Vac. Sci. Technol. A6, 1963 (1988).

14. B. S. Swartzentruber, Y.-W. Mo, M. B. Webb, and M. G. Lagally, J. Vac. Sci. Technol. A7, 2901 (1989).
15. F. K. Men, W. F. Packard, and M. B. Webb, Phys. Rev. Letters 61, 2469 (1988).
16. B. S. Swartzentruber, Y.-W. Mo, M. B. Webb, and M. G. Lagally, J. Vac. Sci. Technol. A8, 210 (1990).
17. T. Sakamoto, K. Sakamoto, K. Miki, H. Okumura, S. Yoshida, and H. Tokumoto, this volume.
18. Handbook of Thin-Film Technology, L. I. Maissel and R. Glang eds., McGraw-Hill, New York, NY (1970).
19. Y.-W. Mo, R. Kariotis, B. S. Swartzentruber, M. B. Webb, and M. G. Lagally, J. Vac. Sci. Technol. A8, 201 (1990).
20. R. Kariotis, Y.-W. Mo, B. S. Swartzentruber, M. B. Webb, and M. G. Lagally, in preparation.
21. Y.-W. Mo and M. G. Lagally, in preparation.
22. R. Hamers, U. K. Köhler, and J. E. Demuth, Ultramicroscopy 31, 10 (1989).
23. E. J. van Loenen, H. B. Elswijk, A. J. Hoeven, D. Dijkkamp, J. M. Lenssinck, and J. Dieleman, this volume; A. J. Hoeven, J. M. Lenssinck, D. Dijkkamp, E. J. van Loenen, and J. Dieleman, Phys. Rev. Letters. 63, 1830 (1989).
24. Y.-W. Mo, B. S. Swartzentruber, R. Kariotis, M. B. Webb, and M. G. Lagally, Phys. Rev. Letters 63, 2393 (1989).
25. C. Herring, Phys. Rev. 82, 87 (1951); in Structure and Properties of Solid Surfaces, R. Gomer and C. S. Smith eds., U. Chicago Press, Chicago (1953).
26. a) D. Saloner, J. A. Martin, M. C. Tringides, D. E. Savage, C. E. Aumann, and M. G. Lagally, J. Appl. Phys. 61, 2884 (1987); b) M. G. Lagally, D. E. Savage, and M. C. Tringides, in Reflection High-Energy Electron Diffraction and Reflection Electron Imaging of Surfaces, P. K. Larsen and P. J. Dobson eds., Plenum, New York (1989); c) P. I. Cohen, G. S. Petrich, A. M. Dabiran, and P. R. Pukite, this volume.
27. R. Kariotis, B. S. Swartzentruber, and M. G. Lagally, J. Appl. Phys. 67, 2848 (1990).
28. M. B. Webb, F. K. Men, B. S. Swartzentruber, R. Kariotis, and M. G. Lagally, this volume.
29. S. Stoyanov, Europhysics Letters, Europhys. Lett. 11, 361 (1990).
30. P. K. Larsen, personal communication.